Error Analyses for the Delivery of a Spinning Probe to Jupiter

Gerald R. Hintz* and James M. Longuski*
Jet Propulsion Laboratory, California Institute of Technology, Pasadena, California

The task of delivering the Galileo Probe to specified atmospheric entry conditions at Jupiter is especially challenging because tracking, trajectory corrections, and attitude adjustments are not possible after release of the Probe from the carrier vehicle. Statistical analyses of the spacecraft dynamics mapped into Probe dispersions in atmosphere-relative and relay-geometry parameters show that attitude stability, heating, and relay performance requirements can be satisfied. Reconstruction techniques are used to enhance estimates of the delivery parameters to permit correct interpretation of the scientific data for the jovian atmosphere. A tradeoff which sacrifices some delivery accuracy and propellant is shown to guarantee satisfaction of a very tight reconstruction requirement for the trajectory considered in this report.

Introduction

THE Galileo Project's carrier spacecraft will release a spinning probe[1] on an entry trajectory into the jovian atmosphere. In preparation for this event, a final trajectory correction maneuver (TCM) will be performed 15 to 50 days before separation and will provide the last adjustment of the atmospheric aimpoint. At 150 days before arrival at Jupiter, the carrier spacecraft will turn to the separation direction (losing communications with the Earth), spinup to 10 rpm to stabilize the inertial attitude, release the Probe along the spin axis, despin to approximately 3 rpm, and finally return to an Earth-pointing attitude to reestablish communications.

Three days after release, another TCM will deflect the carrier craft to overfly the Probe and prepare for insertion into an orbit about Jupiter. Overflight by the carrier vehicle is necessary to receive data during the Probe's descent into the atmosphere for relay to the Earth. No communications with the Probe, other than the reception of scientific data, are possible after its release.

Data are given for a launch early in the 10-day opportunity[2] in May 1986. Delivery conditions for this candidate trajectory are typical because they are determined by the target requirements.

The carrier spacecraft, the Galileo Orbiter, is a dual-spin vehicle. It can operate either in an all-spin mode in which the rotor and stator revolve together, or a dual-spin mode with the stator fixed in inertial space. Dual-spin will be employed, for example, to point the Relay Radio Antenna (RRA) toward the Probe as it descends into the jovian atmosphere as shown in Fig. 1. Most of the propulsive events will be accomplished using twelve 10-N thrusters located in two clusters (of six thrusters each, mounted on separate cantilevered booms) as in Fig. 2. Turns can be performed in a balanced mode in which thrusters are fired as pairs to cancel translational motion introduced by the maneuvers, or they can be used in an unbalanced mode which provides a velocity increment that may be part of a trajectory correction strategy.[3] Three large burns, including the one that deflects the Orbiter away from the entry point, will be performed by a 400-N engine.

Probe Delivery Requirements

There are two phases in the error analyses to meet a priori and a posteriori (reconstruction) requirements. Table 1 specifies the a priori Probe delivery accuracies that satisfy attitude stability, heating, radiation, and "skip out" requirements. Delivery accuracies are measured at the entry point, which is 450 km above the reference ellipsoid at Jupiter. The reference ellipsoid is defined to be at one bar pressure and has an equatorial radius of 71,398 km, while the 450-km altitude is considered to be approximately where sensible aerodynamic forces begin. The relative flight path angle γ_R is the angle between the local horizontal plane and the velocity relative to the jovian atmosphere. The relative angle of attack α_R is the angle between the velocity with respect to the jovian atmosphere and the Probe's spin axis.

The spacecraft attitude at separation is chosen to give a zero relative angle of attack at the point 160 km above the reference ellipsoid where significant atmospheric deceleration forces will be experienced. While 99% dispersions of 4.5 deg about the α_R value at 160-km altitude are acceptable, only 1.9 deg of this tolerance have been allocated to delivery errors caused by uncertainties in position and velocity at separation. The remainder has been allocated to other factors such as separation attitude errors, wobble, nutation, solar pressure, and particle impacts.[4] Although the mission requirement for angle of attack is specified at 160-km altitude, dispersions are computed as for the other parameters at the 450-km entry point for convenience.

The Probe must also be delivered to the 450-km reference altitude at a predetermined epoch and within a specified accuracy to satisfy timing constraints related to the Probe's automatic sequencing activities. For successful Probe to carrier spacecraft (Orbiter) relay link, the Orbiter delivery parameters (shown in Fig. 1) must be controlled at the time of entry such that the 99% statistical error in the Probe aspect angle A_P is less than 3.0 deg and the 99% error in the Orbiter aspect angle A_O is less than 2.0 deg.

The second phase of error analysis responds to a stringent requirement on how well we can reconstruct the entry conditions to permit correct interpretation of the scientific data. This specification is that the 99% uncertainty of the atmosphere-relative flight path angle be within 0.15 deg.

A Priori Error Analyses for Near Separation Events

Trajectory Correction Maneuver

The final TCM before separation will be performed in the Earth-pointing cruise attitude, eliminating turn errors. This TCM is performed in two parts to nullify other maneuver execution errors. That is, a small cleanup maneuver corrects for errors in the larger first burn. The atmospheric aimpoint is adjusted to account for expected velocity increments from the subsequent separation events.

Submitted Dec. 19, 1983; revision submitted June 29, 1984.

*Member of the Technical Staff. Member AIAA.

Turn

The Galileo spacecraft will be turned in the dual-spin mode to the separation attitude. This means turning the angular momentum vector of the combined carrier spacecraft and Probe by a repeated application of torque. The turn will be unbalanced with the $-Z1A$ and $-Z2A$ thrusters (shown in Fig. 2) pulsed alternately every 180 deg, imparting a velocity increment ΔV during the turn.

The probabilistic velocity error model takes into account uncertainties in thrust variation, mass properties, initial spin rate, burn timing, initial attitude, in- and out-of-turn-plane errors, and plume impingement. Flexible body effects and the nutation angle are assumed to be negligible.

The usual spacecraft coordinate system is defined with z along the spin axis and x and y fixed to the rotor or stator, depending on its use. The velocity increment along the direction $\hat{V}_\alpha$ of the spin axis at the midpoint of the turn is[5,6]

$$V_\alpha \approx 2(I_z\omega_z/mr)\sin(\psi/2)$$

where r is the length of the thruster's moment arm, I_z the z component of the moment of inertia, ω_z the z component of the angular velocity, m the carrier/Probe mass, and ψ the turn angle magnitude.

Taking the total differential and dividing by V_α, we have

$$\delta V_\alpha / V_\alpha = \epsilon_{V\alpha} = \epsilon_{Iz} + \epsilon_{\omega z} - \epsilon_m - \epsilon_r + \epsilon_\psi (\psi/2)\cot(\psi/2) \quad (1)$$

where the definition $\epsilon_X = \delta X/X$ has been used throughout and double subscripting has been avoided. Since the expected value of each error source is zero, the standard deviation of Eq. (1) for uncorrelated errors is

$$\sigma_{V\alpha} = [\sigma^2_{\epsilon Iz} + \sigma^2_{\epsilon\omega z} + \sigma^2_{\epsilon m} + \sigma^2_{\epsilon r} + \sigma^2_{\epsilon\psi}(\psi/2)^2\cot^2(\psi/2)]^{1/2} V_\alpha \quad (2)$$

where σ_ϵ denotes the standard deviation in percent for the parameter indicated after the ϵ symbol.

Consider now a system with unit reference vectors $\hat{V}_\alpha$, $\hat{V}_y$ along the turn rotation axis, and $\hat{V}_n$ orthogonal to $\hat{V}_\alpha$ in the rotation plane. For small angles, the total differentials[5] give

$$\sigma_{Vn} = [\sigma^2_{\epsilon 0} + \sigma^2_{\epsilon\psi}\alpha^2]^{1/2} V_\alpha \quad (3)$$

$$\sigma_{Vy} = [\sigma^2_{\epsilon 0} + \sigma^2_{\epsilon\phi}\alpha^2]^{1/2} V_\alpha \quad (4)$$

where $\alpha = \psi/2$ and ϵ_0, ϵ_ψ, and ϵ_ϕ are the nondimensional errors for the initial pointing, turn magnitude, and pointing control during the turn. The error models in Eqs. (3) and (4) take into account fixed errors in ϵ_0 and linear errors in ϵ_ψ and ϵ_ϕ. The first type models such effects as initial attitude uncertainty, thruster mismatch, plume impingement, and turn plane control deadband. The second type is used to model gyro drift errors, or, if gyros are not used for turn control, the growing attitude errors due to timing control. Note that α is proportional to the time, so that terms like $\sigma_\epsilon\alpha$ represent an attitude (gyro) drift.

The values of the Galileo error sources are listed in Table 2 and the resulting velocity components of the execution errors are collected in Table 3. The major error is the uncertainty in the magnitude of V_α determined from Eq. (2). The in-plane and out-of-plane errors normal to V_α are very small.

Table 1 Specifications for Probe delivery conditions

Parameter	Nominal value	Acceptable range (99%)
Relative flight path angle, deg	−8.6	−7.2 to −10.0
Relative angle of attack, deg	0 at 160-km altitude	±4.5 (±1.9 for position and velocity errors at separation)
Time of entry error, min	0	±8
Latitude	1.5°N	5.5°S to 5.5°N, exclusive of the band between 1°S and 1°N
Longitude (System III)[a]	Longitude for minumum radiation dose	±60° from radiation minimum
Relative velocity, km/s	47.4	47.8

[a] System III is a rotational coordinate system for Jupiter that was derived from analysis of radio signals received fom the planet and based on a rotational period of 9 h, 55 min, 29.711 s.

Spinup

Analytic results are available[7] for the solution of Euler's equations of motion and Eulerian angle for near symmetric rigid bodies subject to constant moments. These results provide the angular velocities ω_x, ω_y, and ω_z and the Type 1: 3-1-2 Eulerian angles ϕ_z, ϕ_x, ϕ_y as functions of time. These approximate analytic solutions give highly accurate results when ϕ_x and ϕ_y are small and when the term $|\omega_z|/(|\dot{\omega}_z|\lambda\pi)^{1/2}$ is large. Values greater than 2 for this term give excellent results where

$$\lambda = (\lambda_1\lambda_2)^{-1/2},\ \lambda_1 = (I_z - I_y)/I_x,\ \lambda_2 = (I_z - I_x)/I_y \quad (5)$$

and I_x, I_y, and I_z denote the components of the moment of inertia.

Table 2 Error source data

Error source[a]	Nominal value	99% (2.576σ) A priori error	99% (2.576σ) Reconstructed error
Turn			
I_z	4627 kg-m^2	1.0%	1.0%
ω_z	0.33 rad/s	0.04%	0.04%
Mass	2193 kg	0.4%	0.4%
Length of moment arm	2.085 m	0.08%	0.08%
Initial pointing error	0 mrad	1.0 mrad	1.0 mrad
In-plane turn angle	12.9°	36 mrad	36 mrad
Out-of-plane turn angle	0°	13 mrad	13 mrad
Spinup			
Force	10 N	4.3%	4.3%
Mass	2193 kg	0.4%	0.4%
Initial spin rate	0.306 rad/s	0.04%	0.04%
z-component of plume impingement	0.0220 N	86%	86%
Duration of spinrate change	263.74 s	0.003%	0.003%
z-component of thruster misalignment	0 mrad	8.0 mrad	8.0 mrad
Wobble angle	0 mrad	7.5 mrad	1.9 mrad
Initial phase angle ϕ_{z0}	0 mrad	π rad	30 mrad

[a] The spacecraft mass properties, spin rate, length of moment arm, and force are assumed to be constant during the burns.

Table 3 99% Execution uncertainties, mps

Event	Axis	Delivery uncertainties	Reconstructed uncertainties
Turn	V_n	0.0003	0.0003
	V_α	0.003	0.003
	V_y	0.0001	0.0001
Spinup	V_X	0.020	0.005
	V_Y	0.020	0.005
	V_Z	0.015	0.011
Separation	Normal to V_Z	0.015	0.015
	V_Z	0.022	0.008

To complete the analysis of these maneuvers, a set of differential equations must be integrated, i.e., those corresponding to the ΔVs imparted to the spacecraft during the spinup and spindown.

Let (f_x, f_y, f_z) be the body-fixed forces due to the spin thrusters and m the mass. Then the acceleration components in inertial space are

$$\begin{bmatrix} a_X \\ a_Y \\ a_Z \end{bmatrix} = A \begin{bmatrix} f_x/m \\ f_y/m \\ f_z/m \end{bmatrix} \tag{6}$$

in terms of the transformation matrix A defined in Ref. 8. During the spinup maneuver, the terms f_x, f_y and ϕ_z can be large. Note that f_z is a small term (encompassing thruster misalignment, plume impingement and wobble angle) and that ϕ_x and ϕ_y are also small.[7] By retaining first order terms and neglecting second order and smaller, Eq. (6) becomes

$$a_X = (f_x/m)\cos\phi_z - (f_y/m)\sin\phi_z$$

$$a_Y = (f_x/m)\sin\phi_z + (f_y/m)\cos\phi_z$$

$$a_Z = -(f_x/m)\phi_y + (f_y/m)\phi_x + (f_z/m) \tag{7}$$

Transverse Velocities and Error Model

The transverse components of the inertial velocity, V_X and V_Y, are obtained by integrating the first two equations of Eq. (7). The solution[7] of ϕ_z at time t is

$$\phi_z = (M_z/2I_z)t^2 + \omega_{z0}t + \phi_{z0} = (at^2/2) + bt + \phi_{z0} \tag{8}$$

where M_z is the z component of the moment about the center of mass.

Assuming zero initial conditions, the solutions for V_X and V_Y are

$$V_X = \int_0^t a_X ds = (f_x/m)\tilde{C} - (f_y/m)\tilde{S}$$

$$V_Y = \int_0^t a_Y ds = (f_x/m)\tilde{S} + (f_y/m)\tilde{C} \tag{9}$$

where

$$\tilde{C} = \int_0^t \cos[(as^2/2) + bs + \phi_{z0}]\,ds \tag{10a}$$

$$\tilde{S} = \int_0^t \sin[(as^2/2) + bs + \phi_{z0}]\,ds \tag{10b}$$

The transverse velocity integrals can be solved, using first order asymptotic expansions for the Fresnel integrals[9] in terms of elementary functions to give:

$$V_X \approx (f_x/m)(\omega_z^{-1}\sin\phi_z - \omega_{z0}^{-1}\sin\phi_{z0}) - (f_y/m)(-\omega_z^{-1}\cos\phi_z + \omega_{z0}^{-1}\cos\phi_{z0})$$

$$V_Y \approx (f_x/m)(-\omega_z^{-1}\cos\phi_z + \omega_{z0}^{-1}\cos\phi_{z0}) + (f_y/m)(\omega_z^{-1}\sin\phi_z - \omega_{z0}^{-1}\sin\phi_{z0}) \tag{11}$$

Consider the specific value $\phi_z(0) = \phi_{z0} = 0$. Then, for long spinup durations, the transverse velocities V_X and V_Y in Eq. (11) approach

$$V_X^\infty = \lim_{t\to\infty} V_X = -f_y/(m\omega_{z0})$$

$$V_Y^\infty = \lim_{t\to\infty} V_Y = f_x/(m\omega_{z0}) \tag{12}$$

respectively. The magnitude of the vector

$$\tilde{\rho}(t) = (\Delta V_X, \Delta V_Y) = (V_X - V_X^\infty, V_Y - V_Y^\infty)$$

is

$$\rho(t) = f/(m\omega_z(t)) \tag{13}$$

where $f = (f_x^2 + f_y^2)^{1/2}$. The magnitude $\rho(t)$ shrinks inversely with the current spin rate $\omega_z = \omega_z(t)$, spiralling inward to the limit point (see Fig. 3). Equation (11) shows that $\tilde{\rho}(t)$ is a

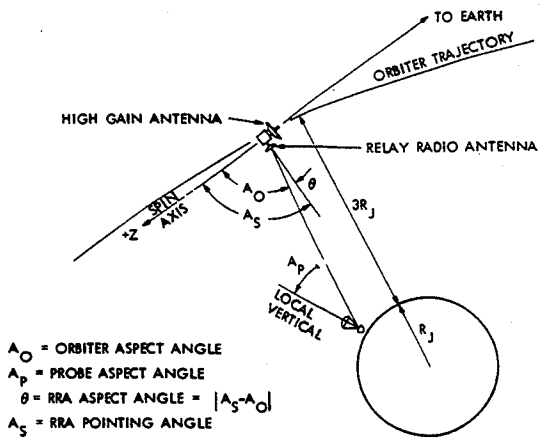

Fig. 1 Relay geometry.

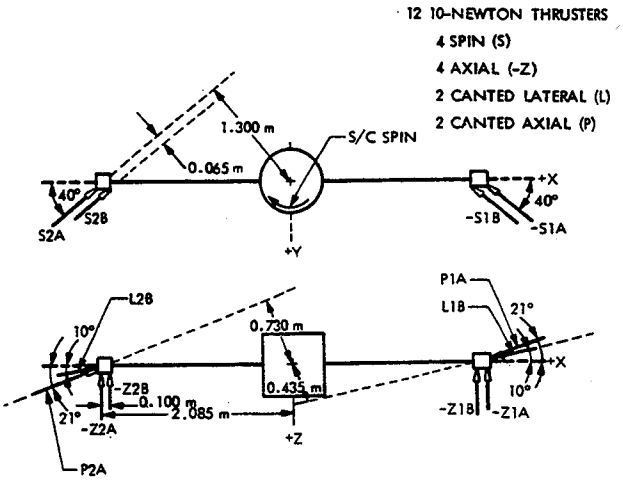

Fig. 2 Thruster configuration on the Orbiter.

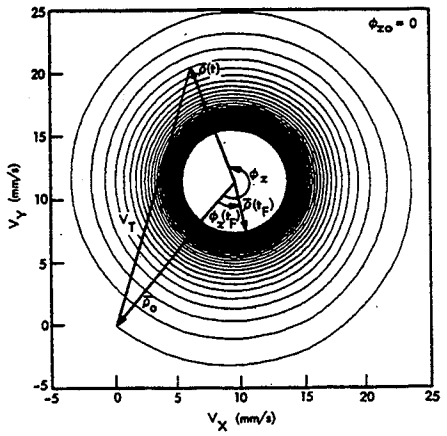

Fig. 3 Transverse velocities during the spinup maneuver.

rotation of the initial vector $\hat{\rho}_0$ through ϕ_z, where $\hat{\rho}$ denotes a unitized vector. Hence, $\phi_z(t)$ is the phase angle between $\bar{\rho}(0)$ and $\bar{\rho}(t)$ at time t.

Actually, the initial phase angle ϕ_{z0} is not known when the spinup begins because it cannot be predicted through the turn or transmitted to Earth. After the spinup maneuver is accomplished, the value of ϕ_{z0} can be reconstructed from telemetry data. Also, the value $\phi_z(t_F)$ at the end of the spinup is not known because the 99% uncertainties in M_z and I_z are about 5% which results in an a priori uncertainty in $\phi_z(t_F)$ of more than 2π radians.

The magnitude of the transverse velocity is obtained from Eq. (11) as

$$V_T = (V_X^2 + V_Y^2)^{1/2}$$

$$= (f/m)\,[\omega_{z0}^{-2} + \omega_z^{-2} - 2\omega_{z0}^{-1}\omega_z^{-1}\cos(\phi_z - \phi_{z0})\,]^{1/2} \qquad (14)$$

Even though the values of ϕ_{z0} and ϕ_z are not known, the largest possible value of $V_T(t_F)$ and the limit of V_T as $t \to \infty$ can be determined as

$$(V_T(t_F))_{\max} = (f/m)\,(\omega_{z0}^{-1} + \omega_{zF}^{-1}) \qquad (15)$$

$$\lim_{t\to\infty} V_T = fm^{-1}\omega_{z0}^{-1} \qquad (16)$$

The error model is derived from Eq. (16), which also represents the mean value of V_T. Perturbing this equation gives

$$V_T(1+\epsilon_{VT}) = (f+\delta f)/[\,(m+\delta m)(\omega_{z0}+\delta\omega_{z0})\,]$$

$$\times\ fm^{-1}\omega_{z0}^{-1}(1+\epsilon_f-\epsilon_m-\epsilon_{\omega z0})$$

For uncorrelated errors with zero mean, the mean and standard deviation are

$$\mu_{VT} = \rho_0 = fm^{-1}\omega_{z0}^{-1}$$

$$\sigma_{VT} \equiv \sigma_{\rho_0} = (\sigma_{\epsilon f}^2 + \sigma_{\epsilon m}^2 + \sigma_{\epsilon\omega z0}^2)^{1/2} fm^{-1}\omega_{z0}^{-1} \qquad (17)$$

where the σ_ϵs are in percent. The total 99% error is given by

$$R = \rho_0 + \rho_F + 2.576\sigma_{\rho 0} \qquad (18)$$

Hence, it is 99% probable that the transverse velocity will lie between the dashed circles illustrated in Fig. 4. This type of error model is discussed in Ref. 10.

Axial Velocity and Error Model

The axial velocity imparted during the spinup is obtained from Eq. (7) as

$$V_Z = -(f_x/m)\int_0^t \phi_y ds + (f_y/m)\int_0^t \phi_x ds + (f_z/m)t + V_{Z0} \qquad (19)$$

Since the integrals in Eq. (19) are small (even though f_x and f_y are not) and the f_z term dominates for large spinup durations,

$$V_Z = (f_z/m)t \qquad (20)$$

where a zero initial value is assumed. The errors are uncorrelated with zero mean so that the mean is

$$\mu_{VZ} = V_Z \qquad (21a)$$

and the standard deviation is

$$\sigma_{VZ} = (\sigma_{\epsilon fz}^2 + \sigma_{\epsilon m}^2 + \sigma_{\epsilon t}^2)^{1/2} V_Z \qquad (21b)$$

which is obtained in the same manner as Eq. (17). Note that when the expected value of f_z is zero a different error model should be used. That is,

$$V_Z = (\epsilon_{fz}/m)t \qquad (22)$$

where

$$\mu_{VZ} = 0, \qquad \sigma_{VZ} = (\sigma_{fz}/m)t \qquad (23)$$

There are three main contributors to the axial acceleration: plume impingement along the z direction, thruster misalignment, and wobble angle. The plume impingement model in Eq. (21) gives $\mu_{VZP} = 0.003$ mps and $\sigma_{VZP} = 33\%$ or 0.001 mps with the uncertainty in the impinging force being the dominant uncertainty (see Table 2). Thruster misalignment in the z direction (3.09 mrad for one standard deviation) provides $\sigma_{VZM} = 0.004$ mps from Eq. (23). The wobble angle, which is the misalignment between the geometric axes of the spacecraft and the principal axes (about which the vehicle tends to spin), has a standard deviation of 2.91 mrad, providing $\sigma_{VZW} = 0.004$ mps.

The final mean of the axial velocity is found by summing the means, which in this case is just the plume impingement effect. The final standard deviation is the square root of the sum of the squares of the standard deviations. For Galileo, the three error sources combine to a 99% dispersion of 0.015 mps with thruster misalignment and wobble angle being the most important. Negligible effects include the plume impingement in the body-fixed x and y directions, because these forces are much smaller than those of the thrusters, and the dynamic wobble angle effects, because they are small and tend to damp down to the equilibrium wobble which is essentially product-of-inertia wobble.

Probe Separation

The Probe will be released mechanically by a spring that will provide a separation velocity of $\Delta V_{SEP} = 0.32$ mps to within 99% tolerances of 26 mm/s along the spin axis and 17 mm/s in a radial (perpendicular to z) direction. In inertial space, these specifications decompose to:

$$[m_P/(m_O+m_P)]\Delta V_{SEP} \text{ for the Orbiter and}$$

$$[m_O/(m_O+m_P)]\Delta V_{SEP} \text{ for the Probe} \qquad (24)$$

from conservation of linear momentum. The allocated values are $m_P = 335$ kg for the mass of the Probe and $m_O = 1858$ kg for the mass of the Orbiter at separation, giving Probe perturbations as in Table 3.

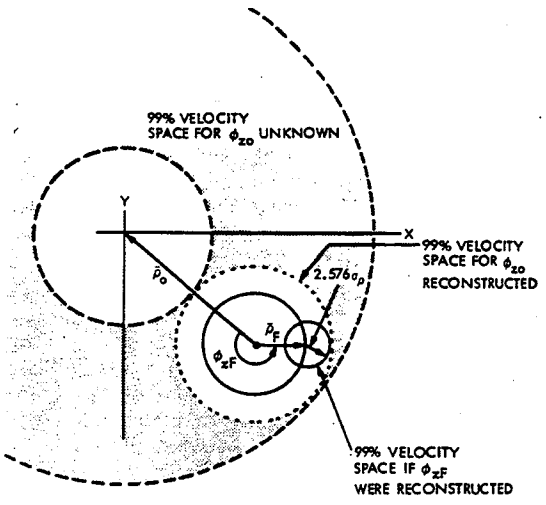

Fig. 4 Velocity error model for the spinrate-change maneuver.

A Priori Probe Delivery Accuracies

Trajectory Correction Maneuver Perturbations

The TCM errors are negligible when compared to the orbit determination (OD) uncertainties[11] incurred when the maneuver parameters are calculated.

Turn Peturbations

The spacecraft will turn from the initial position spin axis direction $\hat{Z}_0$ to the separation direction $\hat{V}_1$. Hence, the covariance of execution errors in (noninertial) spacecraft coordinates is

$$\Lambda_{S/C} = \begin{bmatrix} \left(\frac{0.0003}{2.576}\right)^2 & 0 & 0 \\ 0 & \left(\frac{0.003}{2.576}\right)^2 & 0 \\ 0 & 0 & \left(\frac{0.0001}{2.576}\right)^2 \end{bmatrix}$$

for the selected trajectory with the turn magnitude $\psi = 12.9$ deg (see Eqs. (2-4) and Table 3).

This covariance is mapped to a delivery covariance at entry in a three-step process that accounts for the spacecraft orientation as

$$\Lambda_{\text{TURN}} = MR_{\text{vel}}R_{S/C}\Lambda_{S/C}R_{S/C}^T R_{\text{vel}}^T M^T \tag{25}$$

In this equation, $R_{S/C}$ rotates $\Lambda_{S/C}$ from the $(\hat{V}_{n_2}, \hat{V}_\alpha, \hat{V}_y)$ system to an intermediate reference frame $(\hat{V}_1, \hat{V}_2, \hat{V}_3)$ where $\hat{V}_2$ and $\hat{V}_3$ are selected to be orthogonal to $\hat{V}_1$. Then R_{vel} which has column vectors $\hat{V}_1, \hat{V}_3 = \hat{V}_1 \times \hat{Z}_0 / |\hat{V}_1 \times \hat{Z}_0|$, and $\hat{V}_2 = \hat{V}_3 \times \hat{V}_1$ in Earth mean equator and equinox of 1950.0 coordinates (EME50), continues the rotation by transforming the covariance to an inertial system. Finally, the matrix M contains partial derivatives of the entry parameters with respect to EME50 velocity space variables at separation. The entry parameters of interest are those in Table 1 (for which specifications have been identified), plus the Orbiter and Probe aspect angles. The relative parameters are defined with respect to the atmosphere-relative velocity $\bar{V}_R$ at 450-km altitude. The vector

$$\bar{V}_R = \bar{V} - \bar{V}_A = \bar{V} - (\pi/180)\omega_A R\cos\delta(\hat{P}_N \times \bar{R}) / |\hat{P}_N \times \bar{R}| \tag{26}$$

where $\bar{V}$ is the Probe's inertial velocity, $\bar{V}_A$ the atmospheric velocity, ω_A the spin rate of Jupiter, δ the Probe's declination at position $\bar{R}$, and $\hat{P}_N$ the planet's north pole vector.

The partial derivatives in M are computed as central differences using increments equal to the largest 99% velocity error of 0.022 mps to enhance the accuracy of computing the 99% dispersion level for entry parameters. (M is used for mapping errors for each of the events turn, spinup and separation.) The validity of the linear model in Eq. (25) was verified by varying the size of the increment from 0.01 to 0.04 mps and showing that forward differences changed by less than 2% from the partials for 0.022 mps.

Spinup and Separation Perturbations

Spinup and separation errors are described in a spacecraft body-fixed system above. The spacecraft z-axis is along the separation direction $\hat{V}_1$ for each of these events. Since the reference directions perpendicular to z are unknown, the larger of the dispersions in these directions is used to follow the analysis for a circular distribution. Then $\hat{V}_2$ and $\hat{V}_3$ are chosen to be the spacecraft $\hat{x}$ and $\hat{y}$ coordinates at the epoch of each event.

The covariance of execution errors for these events (see Table 3 for data) map to delivery covariances at entry, Λ_{SPINUP} and Λ_{SEP}, via the three-step process in Eq. (25). However, the rotation matrix $R_{S/C}$ reduces to the product of two elementary matrices as follows:

$$R_{S/C} = \begin{bmatrix} 1 & 0 & 0 \\ 0 & 0 & 1 \\ 0 & 1 & 0 \end{bmatrix} \begin{bmatrix} 0 & 0 & 1 \\ 0 & 1 & 0 \\ 1 & 0 & 0 \end{bmatrix} = \begin{bmatrix} 0 & 0 & 1 \\ 1 & 0 & 0 \\ 0 & 1 & 0 \end{bmatrix}$$

Delivery Accuracies

Thus, a delivery (entry) covariance is obtained for each of the three near separation events. Since these error sources are independent, their covariances can be combined with that of the orbit determination experienced at the TCM by addition. Hence, the delivery covariance is the sum of entry covariances for each of the events as

$$\Lambda_{\text{DEL}} = \Lambda_{\text{OD}} + \Lambda_{\text{TURN}} + \Lambda_{\text{SPINUP}} + \Lambda_{\text{SEP}} \tag{27}$$

The 99% dispersions are then 2.576 σ values in Λ_{DEL}.

The execution uncertainties in Table 3 are mapped to delivery for a candidate trajectory (Table 4) early in the launch window by Eqs. (25) and (27). Sensitivity data, including the M matrix, are given in Table 5 and the resulting 99% delivery dispersions are in Table 6.

Table 5 shows that the gradients of the relative flight path angle, relative angle of attack, and relative velocity are parallel and at an angle of only 14 deg to the separation direction. Hence, velocity errors made along the separation direction produce near maximum dispersions in these three important delivery parameters. At the same time, these parameters are not sensitive to errors along the spacecraft $\hat{x}$ and $\hat{y}$ because these axes are nearly perpendicular to the gradients. Therefore, any future efforts to improve these entry parameters by reducing velocity perturbations (in the delivery or reconstruction analysis phase) must concentrate on errors made along the separation direction.

Table 4 Entry parameters for candidate Probe trajectory

Entry parameter	Value
Latitude, deg	2.2
Longitude, deg (System III)	242.0
Time of entry[a], h:min:s ET on 08/25/88	22:44:00
Relative velocity, km/s	47.396
Hyperbolic excess velocity, km/s (excluding J_2 effects)	5.808
Relative flight path angle, deg	−8.6
Relative angle of attack, deg[a]	0.8
Altitude, km	450
Probe aspect angle, deg	9.6
Orbiter aspect angle, deg	77.6

[a] Zero relative angle of attack occurs 44 s after the 450-km altitude point. ET denotes ephemeris time.

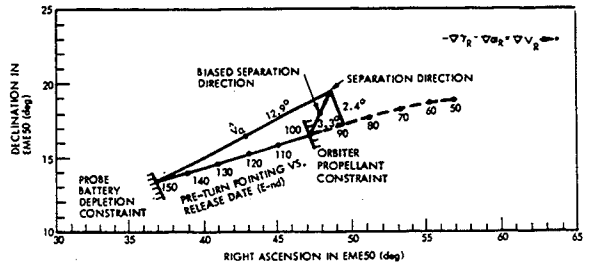

Fig. 5 Turn magnitude variations versus probe release date.

Probe Delivery Reconstruction

Reconstructed Execution Errors

Since it is not possible to track the Probe after separation to determine its trajectory, it is important to reconstruct the velocity increments imparted in the events near separation, especially the spinrate changes and separation. Telemetry data, including attitude, spinrate and accelerometer data, recorded on the Orbiter and played back after its return to Earth pointing can be used in this process.

For convenience, the reconstructed initial value ϕ_{z0} at the spinup is set to zero, which is equivalent to picking the inertial coordinate frame to be the spacecraft x, y, z system when the spinup begins. Then the center of the spiral, $-\rho(0)$, and the final radius of the velocity vector from the center, $\rho(t_F)$, are known. The error model for the transverse velocity vector consists of a mean value, given by the center, $-\bar{\rho}(t_0)$, plus a standard deviation of the center, $\sigma_{\rho 0}$, plus a uniform ring distribution of radius ρ_F as in Fig. 4. Hence, the transverse velocity vector is with 99% probability within a circle of radius R about the average velocity vector $-\bar{\rho}(0)$, where R is as in Eq. (18) with the first term omitted. The reconstructed values, therefore, obtain the 75% improvement from the a priori estimates that are shown in Table 3. However, the more important axial values are only enhanced by 20%.

The Probe separation velocity in the spacecraft z direction can be reconstructed primarily from accelerometer telemetry data. Mass and velocity measurement uncertainties are included in the error model as

$$\sigma_{\Delta VP} = (\sigma_{mO}^2 + \sigma_{mP}^2 + \sigma_{\Delta VO}^2)^{1/2} \Delta V_P \qquad (28)$$

where the Probe's separation velocity is $\Delta V_P = (m_O/m_P)\Delta V_0$ in terms of the velocity increment imparted to the Orbiter. The standard deviations are $\sigma_{mO} = 0.2\%$, $\sigma_{mP} = 0.1\%$, and $\sigma_{\Delta VO} = 1.2\%$, where the accelerometer resolution capability of 0.001 mps is included as a uniformly distributed error and ΔV_O is obtained from Eq. (24). Therefore, the axial velocity of the Probe can be reconstructed to within a 99% uncertainty of 0.008 mps.

Reconstructed Delivery Uncertainties

Miller and Nicholson[11] have shown that Orbiter tracking data through Jupiter encounter can be used to improve the Probe trajectory determination. This process must take into account the execution errors for all events in the separation sequence. When execution uncertainties are reduced using telemetry data, they map into the relative flight path angle via Eq. (25) as in line 2 of Table 7. However, the requirement of ± 0.15 on this entry parameter is not satisfied.

Enhanced Reconstruction

Several techniques are being studied for reconstructing the entry angle. One method takes advantage of the fact that the anti-Earthline (the direction the Probe is pointing before the turn) moves closer to the separation direction after the nominal release time for the trajectory considered in this paper. However, there is a mission engineering constraint to release the Probe by 100 days before entry ($E-100$d) to avoid exceeding the Orbiter propellant budget for its deflection maneuver.[1] By delaying separation to $E-100$d, the turn to

Table 5 Sensitivities of entry parameters to inertial (EME50) velocity perturbations

Entry parameter	∂(entry parameter)/∂(velocity vector), (deg, min or mps)/mps			Magnitude of gradient, (deg, min or mps)/mps	Angle between gradient and separation direction, deg
Latitude, deg	0.0	−0.1	0.5	0.5	79
Longitude, deg	12.7	−16.1	−6.5	21.5	106
Time of entry, min	−34.2	−0.3	−1.5	34.2	130
Relative velocity, mps	132.9	269.4	128.3	326.6	14
Relative flight path angle, deg	−5.1	−10.4	−4.8	12.6	166
Relative angle of attack, deg	2.9	5.9	2.7	7.1	14
Probe aspect angle, deg	−5.8	21.5	9.2	24.1	52
Orbiter aspect angle, deg	−13.8	5.2	1.7	14.8	107

Table 6 Probe 99% a priori delivery dispersions

Entry parameter[a]	Event					
	TCM OD[b]	Turn	Spinup	Separation	Capability	Navigation requirement
Latitude, deg	0.05	−0	0.01	0.01	0.1	0.5
Longitude, deg	2.70	0.06	0.42	0.33	2.8	None
Time of entry, min	4.27	0.07	0.61	0.61	4.4	8
Relative velocity, mps	34.6	0.3	4.9	7.0	35.6	None
Relative flight path angle, deg	0.94	0.01	0.19	0.27	1.0	1.4
Relative angle of attack, deg	0.54	0.01	0.11	0.15	0.6	1.9
Probe aspect angle, deg	2.4	0.06	0.44	0.42	2.5	3.0
Orbiter aspect angle, deg	1.8	0.04	0.29	0.23	1.8	2.0

[a] Dispersions are positive or negative about the nominal value at the 450-km altitude entry point.
[b] TCM errors are essentially orbit determination (OD) uncertainties.

Table 7 Enhancements in 99% relative flight path angle uncertainties, deg

Estimation	Uncertainties from near separation events				Delivery uncertainty	Requirement
	OD	Turn	Spinup	Separation		
A priori	0.94	0.01	0.19	0.27	1.0	1.4
Reconstructed	0.05	0.01	0.14	0.11	0.2	0.15
Reconstructed[a]	0.05	0.01	0.07	0.08	0.1	0.15

[a] For near Earthline separation.

the separation direction is reduced to 3.3 deg as shown in Fig. 5. Now recall that there is a navigation delivery margin of 1.3 deg (shown in Table 6) for the relative angle of attack. Also, S-band communication can be maintained[12] over the high-gain antenna if the boresight is not turned more than 2.1 deg from the Earthline (based on theoretical antenna patterns).

Therefore, delaying the release and biasing the relative angle of attack to be 1.2 deg at 160 km permits taking Doppler information during each of the near separation events. Since separation then is nearly along the Earthline, velocity increments to the Orbiter during spinup and separation can be reconstructed to better than the mm/s level. The axial velocities for spinup and separation can then be reconstructed to within 0.006 mps (99%) via Eq. (28). Also, the sensitivity of the relative flight path angle decreases by one-third from that shown in Table 5 because of the reduced time to go. Thus, 99% variations in the reconstructed value of this entry parameter are reduced to 0.10 deg by trading off 28 mps of Orbit propellant and delivery accuracy in the relative angle of attack.

Conclusions

In conclusion, the following observations can be made:

1) The Probe can be delivered to within the specifications in Table 1 with significant margins.

2) The orbit determination uncertainties of the last trajectory correction maneuver before separation are the dominant source of Probe delivery errors.

3) Spinup and separation give comparable execution (velocity) errors that contribute 0.2 deg or more to the relative flight path angle delivery error. Velocity errors experienced during the turn are nearly insignificant because the turn angles required for the Galileo Mission are small.

4) Reconstruction techniques significantly reduce the a posteriori uncertainty in the specified entry parameter. For the trajectory considered in this paper, the reconstruction requirements can be satisfied by trading off Orbiter propellant and delivery accuracy.

5) Any future efforts to enhance the entry values of the relative flight path angle, relative angle of attack, or relative velocity of the Galileo Probe by reducing velocity perturbations must concentrate on those errors that are along the separation direction.

Acknowledgments

The authors acknowledge many discussions with D.L. Farless concerning Galileo mission design and F.T. Nicholson on orbit determination. Also, the expert computer programming of J.L. Stolzy and D.E. Roth assisted us in the development of the mapping software used in these analyses. The research described in this paper was carried out at the Jet Propulsion Laboratory, California Institute of Technology, under contract with the National Aeronautics and Space Administration.

References

[1] Vojvodich, N.S., Drean, R.J., Schaupp, R.W., and Farless, D.L., "Galileo Atmospheric Entry Probe Mission Description," AIAA Paper 83-0100, Jan. 1983.

[2] D'Amario, L.A. and Byrnes, D.V., "Interplanetary Trajectory Design for the Galileo Mission," AIAA Paper 83-0099, Jan. 1983.

[3] Bantell, M.H., "Control Mode Synthesis for Galileo Spacecraft Maneuvers," AIAA Paper 80-1773, Aug. 1980.

[4] Longuski, J.M. and König, W.W., "A Survey of Non-gravitational Forces and Space Environmental Torques with Applications to the Galileo Spacecraft," AIAA Paper 82-1457, Aug. 1982.

[5] Bantell, M.H., "Considerations for Execution Error Modeling of Galileo Spacecraft Maneuvers," JPL EM 312/79-96 (JPL Internal Document), Nov. 1979.

[6] Longuski, J.M., "Galileo Maneuver Analysis," Paper 81-137, AAS/AIAA Astrodynamics Specialist Conference, Lake Tahoe, Nev., Aug. 1981.

[7] Longuski, J.M., "Solution of Euler's Equations of Motion and Eulerian Angles for Near Symmetric Rigid Bodies Subject to Constant Moments," AIAA Paper 80-1642, Aug. 1980.

[8] Wertz, J.R., *Spacecraft Attitude Determination and Control*, D. Reidel Publishing Co., Boston, Mass., 1978.

[9] Abramowitz, M. and Stegun, I.A., *Handbook of Mathematical Functions*, Dover Publications, Inc., New York, Dec. 1972.

[10] Longuski, J.M. and Kia, T., "A Parametric Study of the Behavior of the Angular Momentum Vector During Spin Rate Changes of Rigid Body Spacecraft," *Journal of Guidance, Control, and Dynamics*, Vol. 7, May-June 1984, pp. 295-300.

[11] Miller, J.K. and Nicholson, F.T., "Galileo Jupiter Approach Orbit Determination," *The Journal of the Astronautical Sciences*, Vol. 32, Jan.-March 1984, pp. 63-80.

[12] Taylor, J.F.H., private communication, June 1983.